Journal of
Materials in Life Sciences

Vol. 5 No. 1 (2026)

Full Paper

Biosynthesis, Characterization and Antifungal Activity of *Moringa oleifera*-Silver Nanoparticles

Nik Ahmad Nizam Nik Malek[ab]*, Qonitatulhaqui Muhamad[a], Muhammad Hariz Asraf[c], Mustapha Isah[d], Hendra Susanto[e], Suhailah Hayaza[f], Happy Kurnia Permatasari[g]

[a]Department of Biosciences, Faculty of Science, Universiti Teknologi Malaysia, 81310 UTM Johor Bahru, Johor, Malaysia.
[b]Centre for Sustainable Nanomaterials, Universiti Teknologi Malaysia, 81310 UTM Johor Bahru, Johor, Malaysia.
[c]HyaNovaX Sdn Bhd, Cubex03, Innovation & Commercialization Centre, Industry Centre, UTM Technovation Park, 81300 Skudai, Johor, Malaysia
[d]Department of Biochemistry, Sokoto State University, Birnin Kebbi Rd, Sokoto 852101, Sokoto, Nigeria
[e]Department of Biology, Faculty of Mathematics and Natural Sciences, Universitas Negeri Malang, Kota Malang, Jawa Timur 65145, Indonesia
[f]Airlangga Functional Nanomaterials Research Group, Faculty of Advanced Technology and Multidiscipline, Universitas Airlangga, Surabaya 60115, Indonesia
[g]Department of Biochemistry and Biomolecular, Faculty of Medicine, Universitas Brawijaya, Malang 65145, Indonesia

Article history
15 January 2026
Revised
11 March 2026
Accepted
21 April 2026
Published online
30 May 2026

*Corresponding author
niknizam@utm.my

Abstract

The development of environmentally friendly approaches to nanoparticle synthesis has attracted increasing interest due to concerns about hazardous chemicals and the energy-intensive nature of conventional methods. In the present study, silver nanoparticles (AgNPs) were successfully synthesized using aqueous leaf extract of Moringa oleifera as a natural reducing and stabilizing agent. The synthesis process was visually confirmed through the gradual colour transformation of the reaction mixture from pale yellow to dark brown, indicating the conversion of silver ions into metallic nanoparticles. UV–Vis spectroscopy revealed a characteristic surface plasmon resonance peak at approximately 480 nm, confirming the formation of AgNPs. Optimal synthesis conditions were determined using 2% plant extract, 1.0 mL extract volume, and 96 h reaction time. Functional group analysis using ATR-FTIR demonstrated the involvement of hydroxyl, carbonyl, and C–O groups from phytochemical constituents in nanoparticle reduction and stabilization. XRD analysis verified the crystalline nature of the synthesized nanoparticles, with diffraction peaks corresponding to face-centred cubic silver. TEM observations showed that the nanoparticles were predominantly spherical with slight agglomeration and an average particle size of 25.235 ± 0.694 nm. The biosynthesized AgNPs also exhibited antifungal activity against *Candida albicans*, where higher nanoparticle concentrations produced larger inhibition zones. The findings suggest that *M. oleifera*-mediated AgNPs possess promising physicochemical and antifungal properties, highlighting their potential for future biomedical and antimicrobial applications.

Keywords : Moringa oleifera, Green synthesis, Silver nanoparticles, Antifungal activity

© 2026 Penerbit UTM Press. All rights reserved

1.0 INTRODUCTION

Invasive fungal infections and fungal contamination have emerged as major global health concerns, particularly in the healthcare, pharmaceutical, food, and environmental sectors. Pathogenic fungi such as *Candida albicans* and *Aspergillus niger* are associated with severe health complications and economic losses due to their ability to contaminate medical devices, food products, and industrial materials. According to the World Health Organization (WHO) Fungal Priority Pathogens List released in 2022, fungal pathogens, including Candida albicans, are categorized among the critical fungal species responsible for severe human infections and increasing antifungal resistance. *C. albicans* is particularly problematic due to its ability to form biofilms on medical devices such as catheters and implants, which enhances resistance toward conventional antifungal therapies and complicates treatment strategies (Parambath et al., 2024). The growing prevalence of antifungal resistance and the limited effectiveness of existing antifungal agents have heightened interest in developing alternative antifungal materials with improved efficacy, biocompatibility, and environmental safety.

Nanotechnology has gained substantial attention in biomedical and environmental applications due to the unique physicochemical properties of nanoparticles, particularly their high surface-area-to-volume ratio, nanoscale size, and enhanced reactivity. Among metallic nanoparticles, silver nanoparticles (AgNPs) have been extensively studied due to their remarkable antimicrobial, antifungal, anticancer, anti-inflammatory, and catalytic properties (Mohd Rozi et al., 2025; Sari et al., 2023). Conventional physical and chemical synthesis methods for AgNPs, however, often involve hazardous chemicals, high energy consumption, and toxic by-products, which limit their environmental compatibility and biomedical applicability. Consequently, green synthesis approaches using biological materials such as plant extracts have emerged as sustainable alternatives for nanoparticle production. Plant-mediated biosynthesis is advantageous because it is cost-effective, eco-friendly, simple, and capable of producing stable nanoparticles without the use of toxic reducing agents (Fatimah et al., 2025; Sari et al., 2023).

Plant extracts contain a wide variety of phytochemicals, including flavonoids, polyphenols, alkaloids, terpenoids, tannins, and saponins, which function as reducing, stabilizing, and capping agents during nanoparticle synthesis. Previous studies have successfully synthesized AgNPs using different plant sources such as *Allium sativum*, *Persicaria odorata*, *Garcinia mangostana*, and *Sida rhombifolia*, demonstrating enhanced antimicrobial, photocatalytic, and biomedical properties (Fatimah et al., 2025; Ismail et al., 2025; Mohd Rozi et al., 2025; Sari et al., 2023). Among these plants, *Moringa oleifera* has attracted increasing interest due to its rich phytochemical composition and diverse pharmacological activities. *M. oleifera* contains bioactive compounds such as flavonoids, phenolic acids, alkaloids, terpenoids, glucosinolates, and polyphenols, which contribute to its antimicrobial, antioxidant, anti-inflammatory, and anticancer activities (Choirunnisa et al., 2025). Recent studies demonstrated that *M. oleifera*-mediated AgNPs were capable of suppressing epithelial–mesenchymal transition (EMT) signaling and inhibiting cervical cancer cell migration, in addition to modulating pAKT and NF-κB pathways to induce apoptosis in HeLa cervical cancer cells (Choirunnisa et al., 2025; Fatiha et al., 2026). These findings further highlight the biomedical potential of *M. oleifera*-derived AgNPs as multifunctional nanomaterials.

In the present study, AgNPs were biosynthesized using *M. oleifera* leaf extract as both reducing and stabilizing agents. The synthesized nanoparticles were characterized using ultra-violet (UV-Vis) spectroscopy, attenuated total reflectance-Fourier transform infrared (ATR-FTIR) spectroscopy, transmission electron microscope (TEM), and X-ray diffraction (XRD) analyses to evaluate their optical, structural, and morphological properties. Furthermore, the antifungal activity of the biosynthesized AgNPs was investigated against *Candida albicans*. This study aims to contribute to the development of environmentally friendly and biologically active nanomaterials with potential applications in antifungal treatment, biomedical technology, and environmental sustainability.

2.0 EXPERIMENTAL

2.1 Biosynthesis of AgNPs

M. oleifera leaf powder used in this study was obtained from the T02 Nanomaterial Laboratory 1, Universiti Teknologi Malaysia (UTM), and supplied by Universal Moringa Plantations, Indonesia. The prepared leaf powder formulation consisted of approximately 400 g of *M. oleifera* leaves, 50 mL of water, and 5 mL of 70% ethanol for every 100 g of the final powder product. The leaf powder was stored in airtight containers at room temperature prior to extraction and nanoparticle synthesis.

The preparation of 5% (w/v) aqueous *M. oleifera* extract was carried out with slight modifications based on previously reported green synthesis methods using plant-mediated AgNPs (Choirunnisa et al., 2025; Fatiha et al., 2026). Approximately 10 g of *M. oleifera* leaf powder was added to 200 mL of ultrapure water and heated at 60°C for 20 minutes using a hotplate equipped with a magnetic stirrer. The mixture was then cooled to room temperature and filtered using Whatman No. 1 filter paper to remove insoluble residues and obtain a clear extract. The filtered extract was stored at 8°C for further use in nanoparticle synthesis.

Optimization of biosynthesized AgNPs was performed by varying the volumes and concentrations of plant extract and the reaction time. The investigated parameters included extract volumes of 0.2, 0.4, 0.6, 0.8, and 1.0 mL, extract concentrations

of 1%, 2%, and 5%, and reaction durations ranging from 0 to 96 hours. A 100 ppm silver nitrate ($AgNO_3$) solution was prepared by dissolving 0.1 g of $AgNO_3$ powder (Sigma) in 1 L of ultrapure water. Subsequently, 10 mL of 100 ppm $AgNO_3$ solution was mixed with the desired volume of plant extract in a test tube and gently stirred to ensure proper interaction between silver ions (Ag^+) and the bioactive compounds present in the extract. The formation of a reddish-brown colour after 24 hours indicated the reduction of Ag^+ ions into metallic AgNPs (Ag^0), consistent with previously reported biosynthesis studies using plant extracts as reducing and stabilizing agents.

The synthesis and optimization of AgNPs were preliminarily evaluated using a Visible Scanning Spectrophotometer (Jenway 7200) over the wavelength range of 380–800 nm, with a scan resolution of 10 nm, in a 2 mL quartz cuvette with a 1 cm path length. Distilled water was used as the blank solution. Based on the optimized surface plasmon resonance (SPR) peak, the synthesis process was repeated using the optimized extract volume and varying extract concentrations.

For large-scale preparation and further characterization, the optimized AgNPs colloidal solution was scaled up to 3 L. The colloidal suspension was centrifuged at 10,000 rpm for 30 minutes using a centrifuge machine (KUBOTA 5922). The supernatant was discarded, and the obtained pellets were washed with ultrapure water by centrifugation at 8000 rpm for 8 minutes to remove impurities and unreacted compounds. The purified AgNPs were dried in an oven at 50°C overnight and subsequently ground using a mortar and pestle to obtain fine AgNPs powder for further analyses (Fatimah et al., 2025; Ismail et al., 2025; Mohd Rozi et al., 2025).

2.2 Characterization techniques

The synthesized AgNPs were characterized using ATR-FTIR, TEM and XRD to evaluate their functional groups, crystal structure, morphology, and particle size. ATR-FTIR analysis was performed in the range of 600–4000 cm^{-1} with a resolution of 4 cm^{-1} and 100 scans to identify the functional groups involved in the reduction and stabilization of AgNPs. The crystalline structure of the AgNPs was analyzed using XRD (Bruker AXS GmBH, Germany) at the University-Industry Research Laboratory (UIRL), UTM. The diffraction patterns were recorded using Cu-Kα radiation (λ = 1.5406 Å) operated at 40 kV and 20 mA over a 2θ range of 5°–50° with a scanning speed of 0.05° s^{-1}. The analysis was conducted to confirm the crystalline nature and phase purity of the synthesized AgNPs (Ismail et al., 2025; Mohd Rozi et al., 2025).

Morphological characterization of the AgNPs was carried out using TEM (Hitachi HT7700) at UIRL, UTM. A drop of AgNPs suspension was placed onto a carbon-coated copper grid and dried before analysis. TEM analysis was used to determine the morphology, particle size, size distribution, and aggregation behaviour of the nanoparticles. The obtained micrographs provided detailed nanoscale information on the synthesized AgNPs (Isah et al., 2025).

2.3 Antifungal assay

The antifungal activity of the AgNPs was investigated against *C. albicans* (ATCC 90028) using the disc diffusion method in accordance with Clinical and Laboratory Standards Institute (CLSI, 2018) guidelines. Potato dextrose agar (PDA) medium and 0.9% saline solution were prepared and sterilized at 121°C for 15 min prior to use. Fresh *C. albicans* colonies were suspended in sterile saline solution, and the turbidity was adjusted to match the 0.5 McFarland standard. The fungal suspension was uniformly swabbed onto PDA plates under aseptic conditions.

AgNPs colloidal solutions were prepared at concentrations of 25, 50, and 100 ppm. Sterile filter paper discs (1.5 cm diameter) were impregnated with 100 µL of each sample and carefully placed onto the inoculated PDA plates using sterile forceps. Econazole and 100 ppm $AgNO_3$ served as positive controls, whereas deionized water and plant extract were used as negative controls. The plates were incubated aerobically at 30–35°C for 24 h. Antifungal activity was assessed by measuring the diameter of inhibition zones formed around each disc. All experiments were conducted in triplicate to ensure reproducibility and reliability of the results (Arsène et al., 2023).

3.0 RESULTS AND DISCUSSION

3.1 Biosynthesis of AgNPs

The biosynthesis of AgNPs using *M. oleifera* leaf extract was monitored through colour observation and UV–Vis spectroscopy analysis to evaluate the effects of extract concentration, extract volume, and reaction time on nanoparticle formation. UV–Vis spectroscopy is commonly used for preliminary confirmation of AgNPs synthesis because it exhibits surface plasmon resonance (SPR) bands in the visible region. The intensity and position of the SPR peak provide important information regarding nanoparticle concentration, particle size, and colloidal stability. Figure 1 shows the colour changes of the colloidal solution over time, and the absorbance intensity at the SPR wavelength of 480 nm. Whereas Figure 2 shows the UV–Vis spectra of AgNPs synthesized under different conditions.

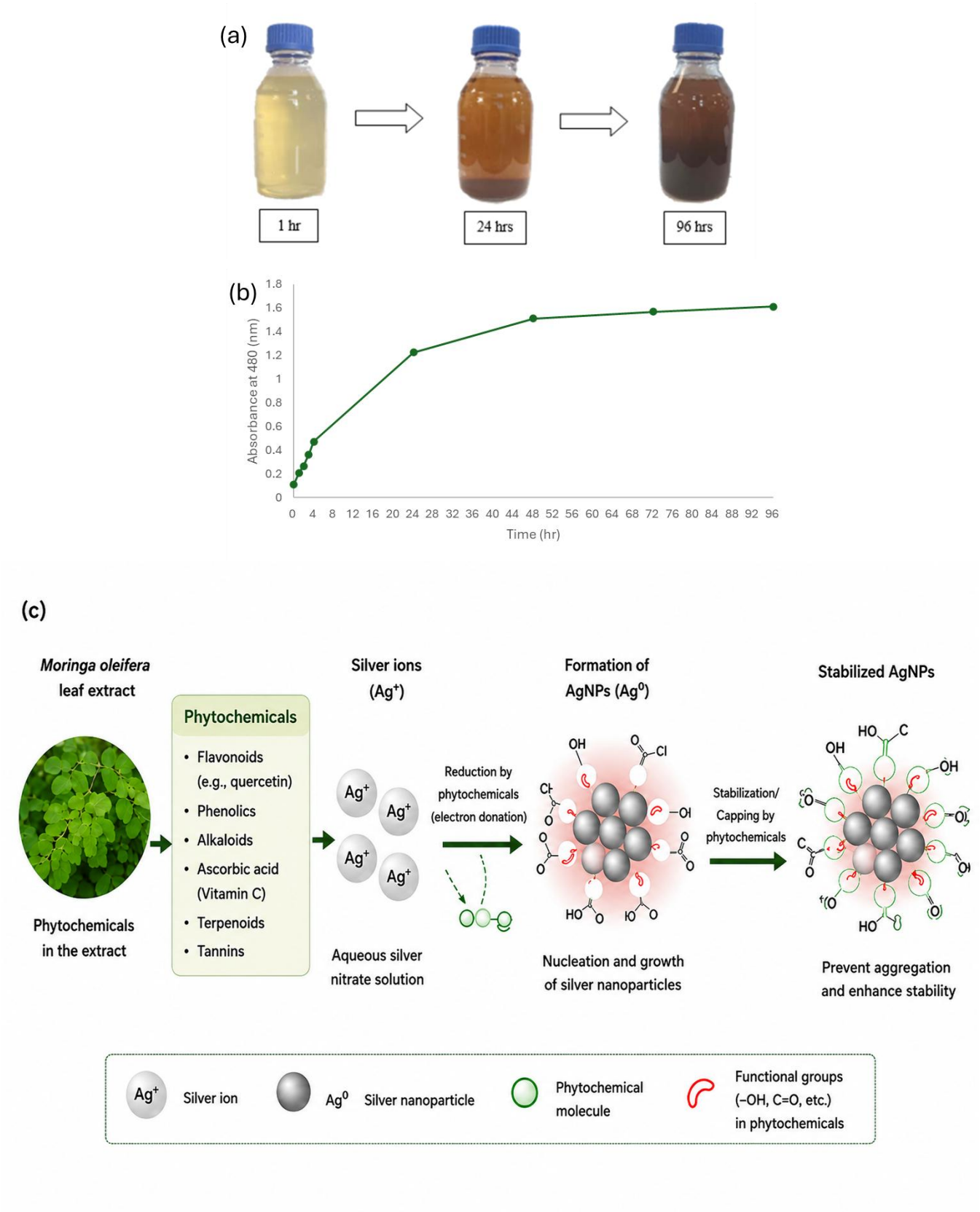


Figure 1: (a) colour changes of AgNPs colloidal solution over time, (b) absorbance intensity of AgNPs at 480 nm with increasing reaction time, and (c) proposed mechanism for the green synthesis and stabilization of AgNPs using *M. oleifera* leaf extract.

The formation of AgNPs was successfully confirmed by visible colour changes and UV–Vis spectroscopy, as shown in Figure 1(a). Initially, the reaction mixture appeared yellowish, but gradually changed to brownish and dark reddish-brown after 24 and 96 hours, respectively (Figure 1a). This colour transformation indicates the reduction of silver ions (Ag^{+}) to metallic AgNPs (Ag^{0}) via the excitation of surface plasmon resonance (SPR) on the nanoparticle surface. Similar observations have been widely reported in green synthesis studies of AgNPs using plant extracts (Din et al., 2022; Mohd Rozi et al., 2025). The reduction process is mainly attributed to the presence of phytochemicals, such as flavonoids, phenolics, alkaloids, and ascorbic acid, in the *M. oleifera* extract, which function as reducing and stabilizing agents during nanoparticle formation (Figure 1(c)). Compounds such as quercetin and vitamin C are known to possess strong electron-donating and metal-chelating properties, facilitating AgNPs synthesis and stabilization.

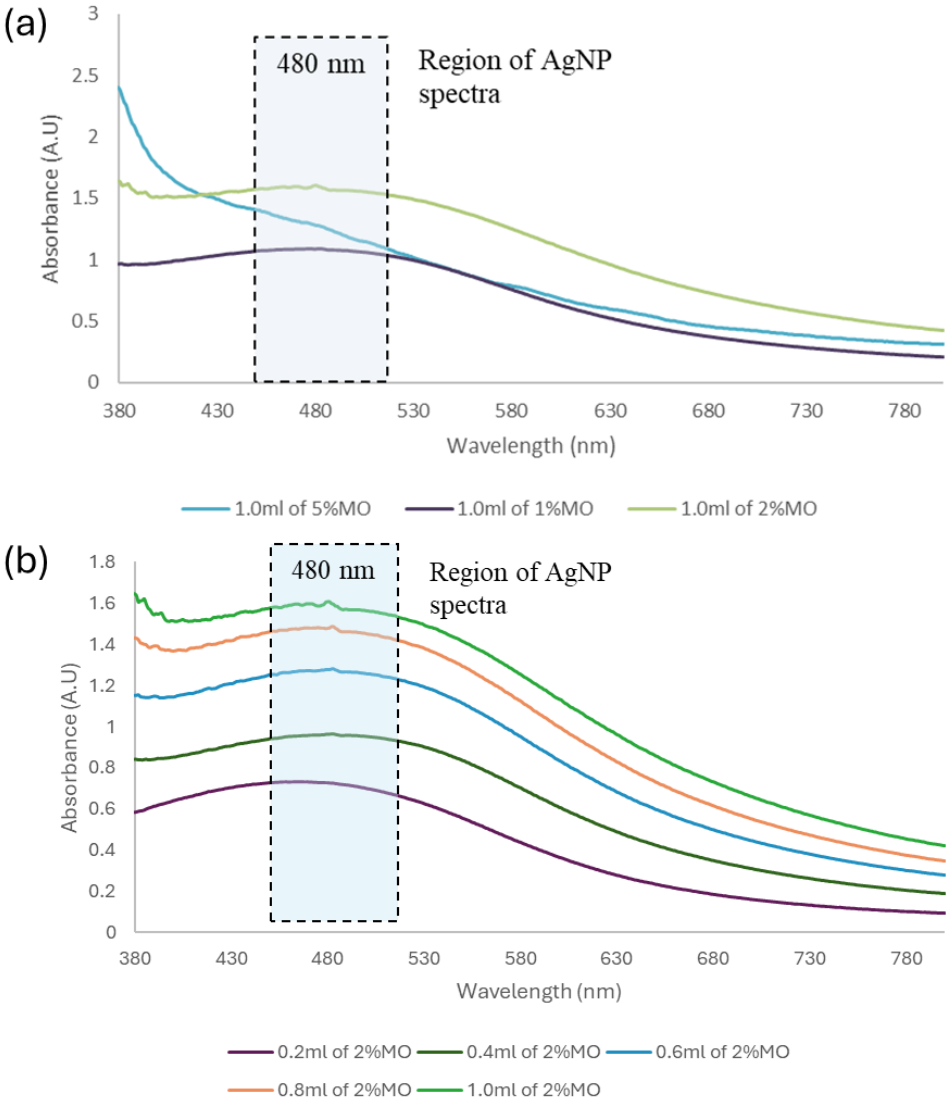


Figure 2 : (a) UV–Vis spectra of biosynthesized AgNPs measured at different concentrations and (b) UV–Vis spectra of biosynthesized AgNPs measured at different extract volumes after 96 hours.

The effect of plant extract concentration on AgNPs formation was evaluated using UV–Vis spectroscopy, as illustrated in Figure 2(a). All synthesized samples exhibited characteristic SPR absorption bands within the range of 450–530 nm, confirming the formation of AgNPs. Among the tested concentrations, the 2% *Moringa* extract produced a more distinct and stable SPR peak centred at approximately 480 nm compared to 1% and 5% concentrations. The 1% extract exhibited a relatively weak, broad absorption peak, suggesting insufficient reducing biomolecules for effective nanoparticle nucleation. In contrast, the 5% extract exhibited broader spectra with less-defined peaks, suggesting possible particle aggregation or excessive phytochemical interactions. The sharper and more defined SPR peak observed for the 2% extract indicates improved nanoparticle formation, better dispersion, and enhanced colloidal stability. Similar trends have been reported in plant-mediated AgNPs synthesis, where moderate extract concentrations produced more stable nanoparticles with controlled size distribution (Fatimah et al., 2025; Sari et al., 2023).

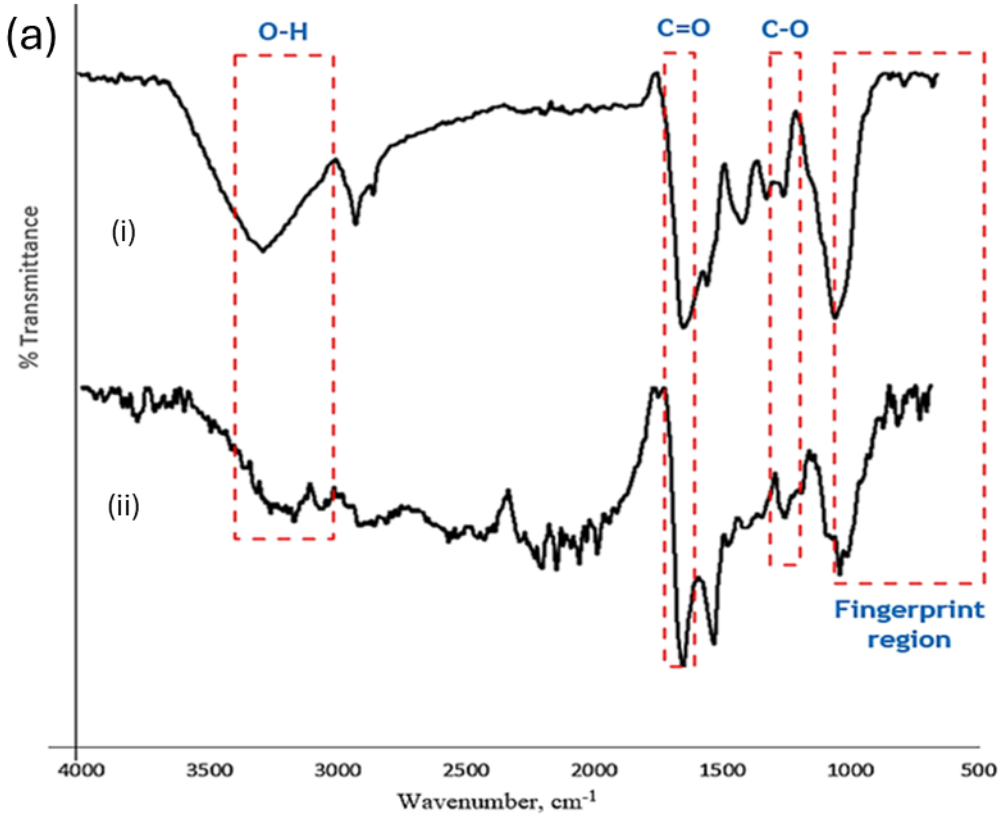
Optimizing the extract volume further demonstrated its significant influence on nanoparticle synthesis, as shown in Figure 2(b). Increasing the extract volume from 0.2 mL to 1.0 mL resulted in progressively higher absorbance intensity at the SPR region around 480 nm. Lower extract volumes (0.2–0.4 mL) produced weaker absorption peaks, indicating lower nanoparticle concentration due to limited reducing and stabilizing compounds. As the volume increased to 0.6–1.0 mL, the absorption peaks became sharper and more intense, suggesting enhanced reduction of Ag^+ ions and improved nanoparticle formation. The highest absorbance intensity was observed at 1.0 mL of 2% *Moringa* extract, indicating that this condition provided sufficient phytochemicals for efficient nucleation, growth, and stabilization of AgNPs. The SPR peak at approximately 480 nm also suggests the formation of relatively spherical nanoparticles with moderate particle size, consistent with previous AgNPs studies using plant extracts (Ismail et al., 2025; Mohd Rozi et al., 2025).

The reaction time study revealed that AgNPs formation increased progressively with increasing synthesis duration, as illustrated in Figure 1(b). The absorbance intensity at 480 nm increased rapidly during the initial hours and continued to rise gradually, reaching its highest value after 96 hours. This indicates a continuous reduction in silver ions and a gradual increase in nanoparticle size over time. The increase in absorbance intensity corresponds to an increase in nanoparticle concentration within the colloidal solution. The relatively stable absorbance after prolonged incubation also suggests good colloidal stability of the synthesized AgNPs, with minimal aggregation. Based on the overall UV–Vis analysis, the optimum conditions for AgNPs synthesis were determined to be 2% *Moringa* extract at 1.0 mL and a reaction time of 96 hours. These optimized parameters produced the highest SPR intensity and the most stable colloidal AgNPs suitable for further characterization and antifungal studies.

3.2 Samples characterization

3.2.1 Structural and bonding characteristics

The successful biosynthesis of AgNPs using *M. oleifera* leaf extract was further verified through ATR-FTIR and XRD analyses. ATR-FTIR analysis was employed to identify the functional groups involved in the reduction and stabilization of the synthesized AgNPs, while XRD analysis was carried out to examine the crystalline structure and phase composition of the nanoparticles. These characterization techniques provided valuable information regarding the interaction between phytochemical compounds present in the *M. oleifera* extract and the formed AgNPs.



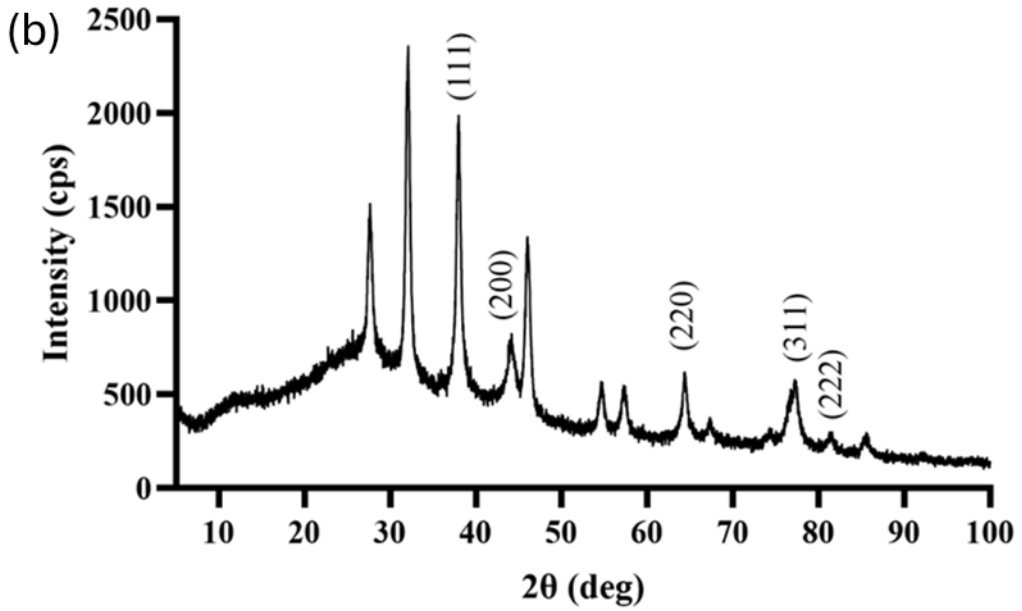


Figure 3 : (a) ATR-FTIR spectra of (i) *M. oleifera* extract and (ii) biosynthesized AgNPs, and (b) XRD pattern of biosynthesized AgNPs.

The ATR-FTIR spectra of *M. oleifera* extract and biosynthesized AgNPs are shown in Figure 3(a). The broad absorption band observed at 3281 cm^{-1} in the plant extract corresponded to O–H stretching vibrations associated with phenolic and alcohol compounds. The peak at 1639 cm^{-1} was attributed to C=O or C=C stretching vibrations, while the absorption band at 1247 cm^{-1} corresponded to C–O stretching vibrations (Kurniawan, 2021; Lubis et al., 2022; Maheshwari et al., 2023). These functional groups are commonly associated with flavonoids, polyphenols, alkaloids, proteins, and other phytochemicals present in *M. oleifera* extract. After nanoparticle synthesis, similar absorption bands were observed in the AgNPs spectrum with slight shifts in peak positions and reduced intensities, particularly at 3162 cm^{-1}, 1628 cm^{-1}, and 1224 cm^{-1}. The observed shifts indicated the involvement of hydroxyl, carbonyl, and phenolic groups in the reduction of Ag^{+} ions and stabilization of the synthesized nanoparticles. These findings suggest that phytochemicals from the *M. oleifera* extract acted as both reducing and capping agents during AgNPs synthesis, preventing excessive nanoparticle aggregation. Similar observations have been reported in previous plant-mediated AgNPs synthesis studies (Fatimah et al., 2025; Sari et al., 2023).

The crystalline structure of the synthesized AgNPs was confirmed through XRD analysis, as shown in Figure 3(b). The XRD diffractogram exhibited distinct diffraction peaks at approximately 37.96°, 44.04°, 64.28°, 77.31°, and 81.22°, corresponding to the lattice planes (111), (200), (220), (311), and (222), respectively (Waiezi et al., 2023). The peak positions and diffraction line intensities matched well with the standard reference of silver (ICDD no. 01–071–4613) in the face-centered cubic (fcc) structure (Kapoor et al., 2022). Among the diffraction peaks, the (111) plane exhibited the highest intensity, indicating preferential crystal orientation and high crystallinity of the synthesized nanoparticles.

The appearance of additional diffraction peaks indicated the presence of biomolecules from *M. oleifera* on the surface of AgNPs. The XRD pattern showed six diffraction peaks, with the most distinct peak at 45.986˚ corresponding to molybdenum oxide. As stated by Mawardi et al. (2020), molybdenum (Mo) is among the most abundant microelements in Moringa grown in the Malang area of East Java, Indonesia, which is the same export destination for the Moringa powder used in this study. In another study by Biel et al. (2017), both extracted and unextracted Moringa contained significant levels of nutrients essential for the proper functioning of organisms, including Mo. During oven drying of samples (50-60˚C, 24 hours) for XRD analysis, which may expose them to oxygen and humidity, a thin layer of molybdenum oxide may form gradually. The organic and inorganic forms of Mo in the Moringa sample could oxidize to form molybdenum oxides (MoO_3). Thus, the unusual peaks in the XRD diffractogram might arise from the high intensity of oxidized Mo in the Moringa itself.

3.2.2 Morphological analysis

Transmission electron microscopy (TEM) analysis was performed to evaluate the morphology, particle size, and dispersion behaviour of the AgNPs. Figure 4 shows TEM micrographs of the synthesized AgNPs at different magnifications, along with the particle size distribution histogram. Based on TEM images, the synthesized nanoparticles were predominantly spherical, with particle sizes distributed throughout the sample. The formation of mostly spherical nanoparticles suggests that the phytochemicals in the plant extract effectively acted as reducing and stabilizing agents during nanoparticle synthesis. Similar spherical morphologies have been commonly reported in green-synthesis studies of AgNPs using plant extracts, due to controlled nucleation and growth mechanisms (Fatimah et al., 2025; Sari et al., 2023). In the study by Fatimah et al. (2025),

AgNPs synthesized using *Sida rhombifolia* extract also exhibited predominantly spherical morphology with good crystallinity. Spherical nanoparticles are generally preferred due to their greater stability, larger surface-area-to-volume ratio, and improved biological interactions, particularly for antimicrobial applications (Mohd Rozi et al., 2025).

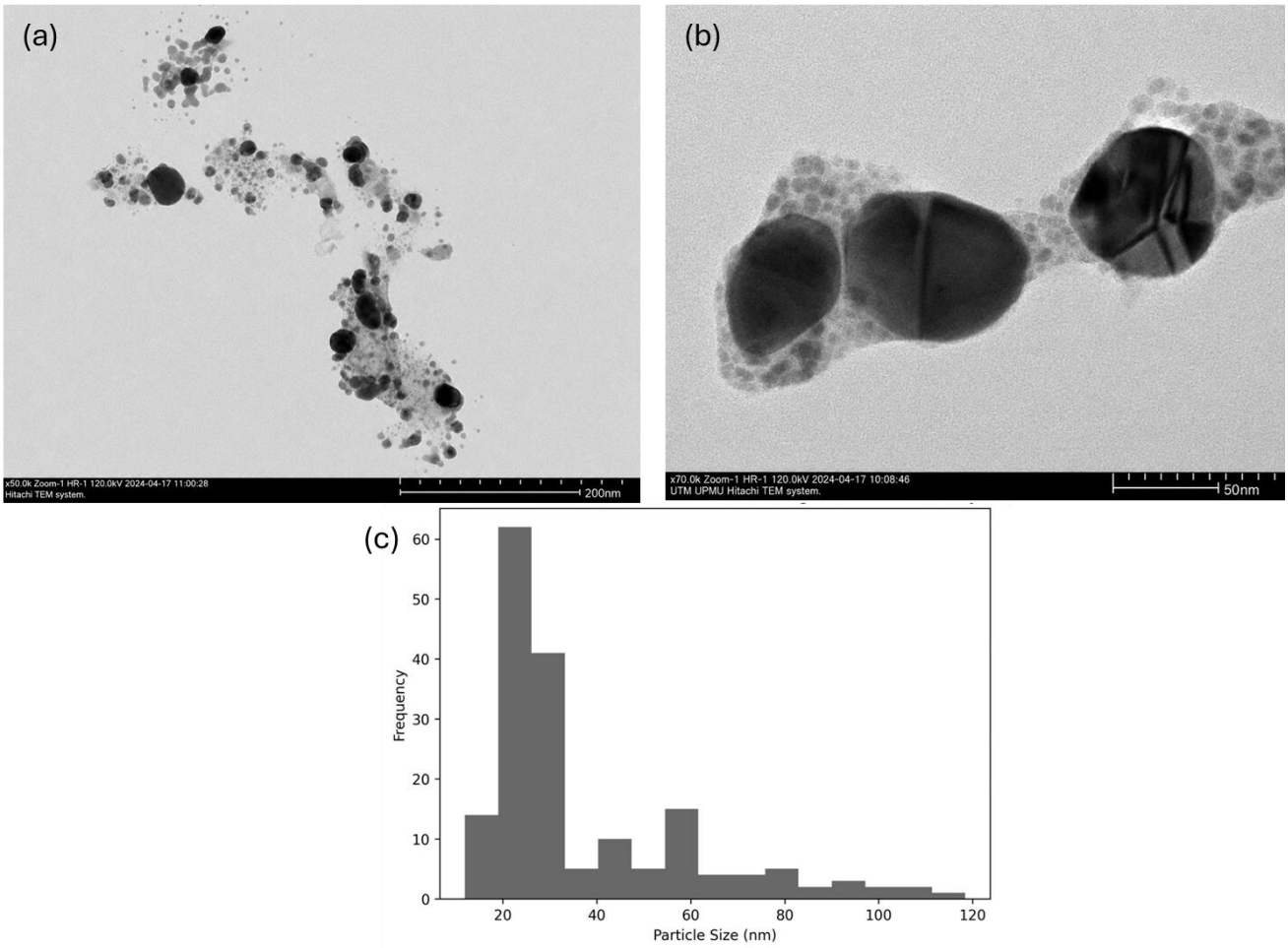


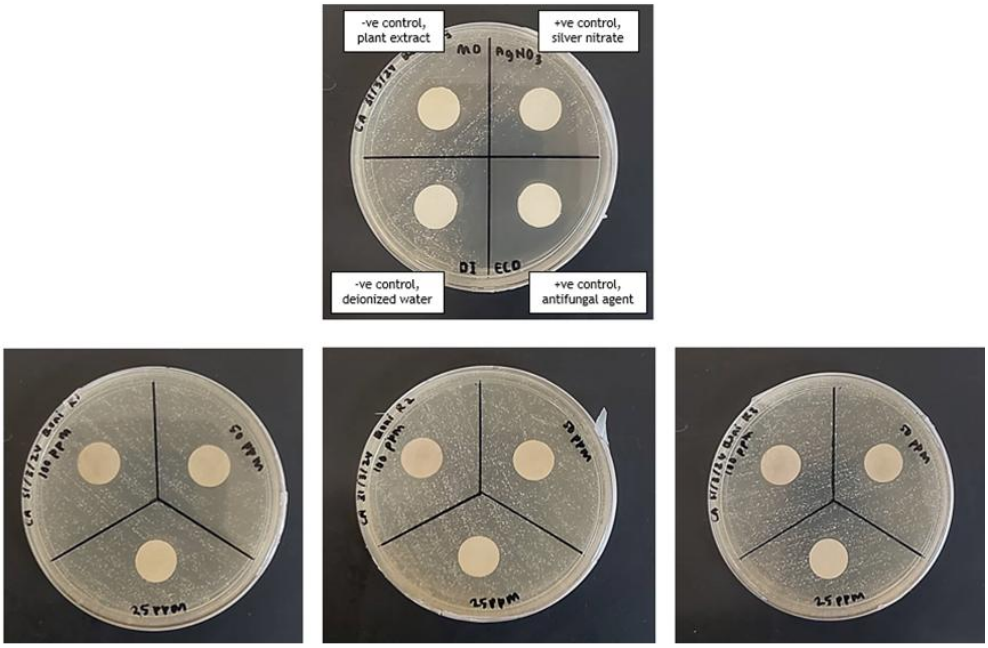
Figure 4 TEM images of biosynthesized AgNPs at (a) 50,000× magnification, (b) 70,000× magnification, and (c) particle size distribution histogram of AgNPs.

The TEM images also revealed that the AgNPs exhibited both dispersed and slightly agglomerated arrangements. Several regions displayed well-dispersed nanoparticles, whereas other areas showed nanoparticle clusters and aggregates. This slight agglomeration may be attributed to particle interactions during centrifugation and sample-drying, which could reduce nanoparticle dispersion stability. Similar aggregation behaviour was also observed in biosynthesized AgNPs reported by Razak et al. (2023), where phytochemical-coated nanoparticles tended to form clusters due to intermolecular interactions between surface-bound biomolecules. Nevertheless, the majority of nanoparticles remained nanosized and uniformly distributed around the surrounding biomolecular matrix. The higher-magnification TEM image further confirmed the presence of nanoscale spherical particles surrounded by lighter organic layers, which may correspond to phytochemical capping agents from the *Moringa* extract that stabilize the nanoparticles.

The particle size distribution histogram in Figure 4(c) indicates that most nanoparticles were distributed in the range of approximately 15–35 nm, with fewer larger particles extending beyond 50 nm due to aggregation. The average particle size of the AgNPs was estimated to be 25.235 ± 0.694 nm, indicating relatively small nanoparticles with a narrow size distribution. Comparable nanoscale particle sizes have also been reported in previous plant-mediated AgNP synthesis studies, including AgNPs synthesized using *S. rhombifolia* extract with an average size of 63.5 nm (Fatimah et al., 2025) and AgNPs synthesized from garlic callus extract with nanosized distributions (Sari et al., 2023). The relatively smaller particle size obtained in the present study suggests efficient reduction and stabilization by the phytochemicals present in the *M. oleifera* extract. Smaller particle sizes are advantageous for antimicrobial and biomedical applications because they provide larger active surface areas and enhanced interaction with microbial cells. Overall, the TEM analysis confirmed the successful biosynthesis of predominantly spherical, nanosized AgNPs with relatively good dispersion and a controlled particle size distribution, suitable for further antifungal applications.

3.3 Antifungal activity

The antifungal activity of the AgNPs against *C. albicans* was evaluated using the disc diffusion assay under optimized conditions. The experiment was conducted in triplicate to ensure the reproducibility and reliability of the results, and no contamination was observed throughout the experimental procedures, indicating proper aseptic handling. Figure 5 presents the inhibition zones formed around discs containing AgNPs at different concentrations, and the table within the figure summarizes the average inhibition zone diameter and its standard deviation. The results demonstrated that AgNPs synthesized using *M. oleifera* extract exhibited antifungal activity against *C. albicans*, particularly at higher nanoparticle concentrations.



Control and sample concentration	Average diameter of inhibition zones (cm) ± standard deviation
Positive control: $AgNO_3$	1.76 ± 0.04
Positive control: Antifungal agent	2.44 ± 0.04
Negative control: Deionized water	0 ± 0
Negative control: Plant extract	0 ± 0
Sample: 100 ppm Bio-AgNPs	1.67 ± 0.05
Sample: 50 ppm Bio-AgNPs	1.63 ± 0.10
Sample: 25 ppm Bio-AgNPs	0 ± 0

Figure 5: Antifungal activity of AgNPs against *C. albicans* using disc diffusion assay after 24 hours of incubation. The top image shows control groups, while the bottom images show AgNPs samples at concentrations of 100 ppm, 50 ppm, and 25 ppm.

The disc diffusion assay revealed clear inhibition zones for AgNPs at concentrations of 100 ppm and 50 ppm, with average inhibition diameters of 1.67 ± 0.05 cm and 1.63 ± 0.10 cm, respectively. In contrast, the 25 ppm AgNPs sample did not produce any detectable inhibition zone, indicating insufficient nanoparticle concentration to suppress fungal growth effectively. The positive control using an antifungal agent exhibited the largest inhibition zone (2.44 ± 0.04 cm), followed by $AgNO_3$ solution (1.76 ± 0.04 cm), while both deionized water and plant extract controls showed no inhibition activity. These findings are supported by Rhozin et al. (2021), who stated that AgNPs exhibit antifungal activity against *C. albicans* by disrupting cell membranes and inhibiting normal cell division. In addition, AgNPs inhibit cellular processes involved in yeast budding, likely by disrupting membrane integrity. Whereas, a recent study by Tailor and Marwal (2026) showed that the AgNP synthesized using *Mangifera indica* flower bud extract also exhibited antifungal activity against *C. albicans*, with an activity of 0.92 ± 0.15 cm, which is lower than that of $AgNO_3$ (1.03 ± 0.33 cm).

The antifungal mechanism of AgNPs may involve disruption of fungal cell membrane integrity, increased membrane permeability, generation of reactive oxygen species (ROS), and interference with intracellular metabolic processes. AgNPs also inhibit yeast budding and cellular division by interacting with membrane proteins and nucleic acids (Rozhin et al., 2021). The relatively small particle size and predominantly spherical morphology observed in the TEM analysis may further enhance the antifungal activity of the AgNPs, as smaller nanoparticles have higher surface-area-to-volume ratios, enabling greater interaction with fungal cell surfaces. The consistent inhibition zones observed across triplicate experiments demonstrate the reproducibility and stability of the synthesized AgNPs.

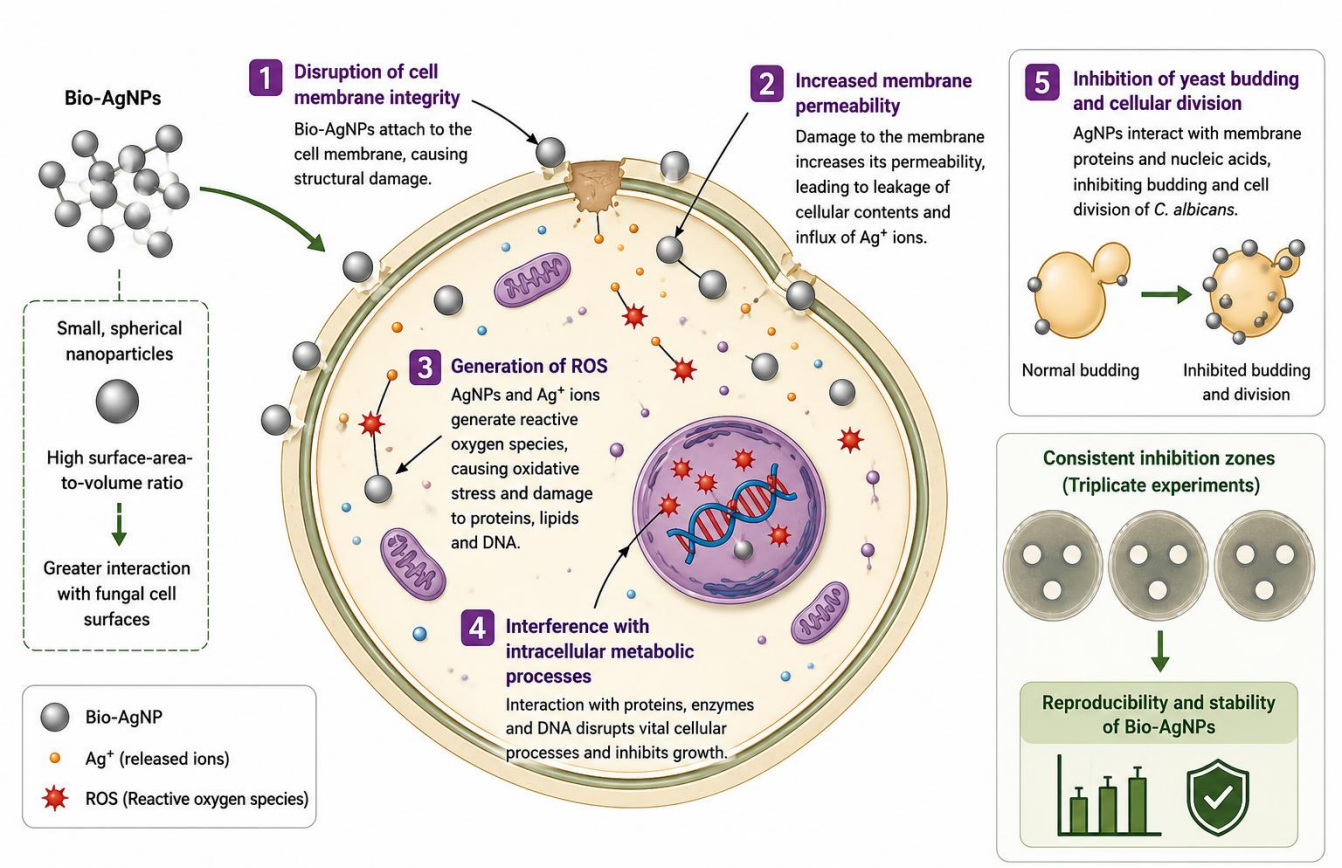


Figure 6: Proposed antifungal mechanism of biosynthesized AgNPs against *C. albicans*.

Figure 6 illustrates the proposed antifungal mechanism of the AgNPs against *C. albicans*. The AgNPs initially interact with the fungal cell surface, disrupting cell membrane integrity and increasing membrane permeability. This interaction may lead to leakage of intracellular contents and facilitate the penetration of silver ions (Ag^+) into the fungal cells. In addition, the AgNPs can stimulate the generation of reactive oxygen species (ROS), which induce oxidative stress and damage essential cellular components, including proteins, lipids, enzymes, and nucleic acids. The nanoparticles may also interfere with intracellular metabolic activities and inhibit normal cellular functions by interacting with membrane proteins and DNA, ultimately suppressing fungal growth and viability (Rozhin et al., 2021). Furthermore, the AgNPs inhibit yeast budding and cellular division, preventing the proliferation of *C. albicans*. The relatively small particle size and predominantly spherical morphology observed in TEM analysis may further enhance the antifungal activity of the AgNPs, as they provide a higher surface-area-to-volume ratio, enabling greater interaction with fungal cell surfaces. The consistent inhibition zones observed in triplicate experiments also indicate the reproducibility, stability, and reliable antifungal activity of the synthesized AgNPs.

4.0 CONCLUSION

In conclusion, biosynthesized AgNPs were successfully produced from *M. oleifera* leaf extract using a green, environmentally friendly approach. The biosynthesized AgNPs exhibited characteristic optical, structural, and morphological properties with predominantly spherical nanoparticles and an average particle size of 25.235 ± 0.694 nm. The biosynthesized AgNPs also demonstrated concentration-dependent antifungal activity against *C. albicans*, highlighting their potential application as sustainable antifungal nanomaterials for biomedical and environmental applications.

Acknowledgment

The authors would like to acknowledge the financial support from the Ministry of Education Malaysia, Universiti Teknologi Malaysia, and Universitas Negeri Malang, Indonesia, under the Matching Grant QJ13000.3009.04M28.

References

1. Arsène, M. M. J., Podoprigora, I. V., Marukhlenko, A., Morozova, M., Senyagin, A. N., Anyutoulou, K. L. D., Mumrova, E. Y., Manar Rehailia, Ada Arsene Gabin, Kulikova, A. A., Yashina, N. V., Zhigunova, A. V., Orlova, S., & Das, M.

(2023). Antifungal activity of silver nanoparticles prepared using Aloe vera extract against *Candida albicans*. Veterinary World, 16(1), 18–26.

2. Biel, W., Jaroszewska, A., & Łysoń, E. (2017). Nutritional quality and safety of *Moringa oleifera* Lam. leaves as an alternative source of protein and minerals. *Journal of Elementology, 22*(2), 569–579.
3. Clinical and Laboratory Standards Institute (CLSI). (2018). Performance standards for antimicrobial susceptibility testing (28th ed.). CLSI supplement M100. Clinical and Laboratory Standards Institute.
4. Choirunnisa, N. L., Kezia, D. C., Permana, A. Z., Malek, N. A. N. N., Nurkolis, F., & Permatasari, H. K. (2025). Modulation of pAKT and NF-κB pathways by *Moringa oleifera* silver nanoparticles: Inducing apoptosis in cervical cancer cells. *CyTA - Journal of Food, 23*(1), 2543878.
5. Din, S. M., Malek, N. A. N. N., Shamsuddin, M., Matmin, J., Hadi, A. A., & Asraf, M. H. (2022). Antibacterial silver nanoparticles using different organs of *Ficus deltoidea* Jack var. kunstleri (King) Corner. *Biocatalysis and Agricultural Biotechnology, 44*, 102473.
6. Fatimah, F., Wahab, A. W., Karim, A., Fauziah, S., Hasanuddin, A. R. P., Rajab, A., Muriyati, M., Islawati, I., & Salnus, S. (2025). Silver nanoparticles-aqueous leaf extract of sidaguri (*Sida rhombifolia*) as reducing agents. *Jurnal Teknologi, 87*(1), 27–33.
7. Fatiha, R. A., Ngabdi, C. K., Azizah, J. S., Putri, B. S. N., Lestari, B., Malek, N. A. N. N., Susanto, H., Riawan, W., & Permatasari, H. K. (2026). Disruption of EMT signaling and migration by *Moringa oleifera* leaf powder-silver nanoparticles (MOLP-AgNPs) in HeLa cervical cancer cells. *Asian Pacific Journal of Cancer Prevention, 27*(3), 981–988.
8. Isah, M., Malek, N. A. N. N., Susanto, H., Asraf, M. H., & Aliero, A. S. (2025). Preparation, characterization, and antibacterial activity of Moringa oleifera-silver nanoparticles-kaolinite nanocomposite. *Applied Clay Science*, *269*, 107761.
9. Ismail, I. Q., Malek, N. A. N. N., Asraf, M. H., & Matmin, J. (2025). Eco-friendly fabrication of *Persicaria odorata*-silver nanoparticles-kaolinite composite and its efficacy as antibacterial agent. *Journal of Materials in Life Sciences, 4*(1), 69–78.
10. Kapoor, S., Sood, H., Saxena, S., & Chaurasia, O. P. (2022). Green synthesis of silver nanoparticles using *Rhodiola imbricata* and *Withania somnifera* root extract and their potential catalytic, antioxidant, cytotoxic and growth-promoting activities. *Bioprocess and Biosystems Engineering*, 45, 365-380.
11. Kurniawan, Y. S. (2021). A comparative study on phytochemical screening and antioxidant activity of aqueous extract from various parts of *Moringa oleifera*. *Indonesian Journal of Natural Pigments, 3*(2), 43–47.
12. Lubis, F. A., Malek, N. A. N. N., Sani, N. S., & Jemon, K. (2022). Biogenic synthesis of silver nanoparticles using *Persicaria odorata* leaf extract: Antibacterial, cytocompatibility, and in vitro wound healing evaluation. *Particuology, 70*, 10–19.
13. Maheshwari, S., Bharti, S., Gusain, A., Khan, S. A., & Matra, N. G. (2023). FT-IR analysis of *Moringa oleifera* L. leaf extract and its insecticidal activity against *Callosobruchus chinensis* L. (Coleoptera: Bruchidae). *Biological Forum – An International Journal, 15*(10), 1047–1051.
14. Mawardi, A. I., Susanto, H., Taufiq, A., Yunisa, D. T., Rufiandita, F., Nizarghazi, F., Alifi, G., & Putri, L. N. (2020). Halal material synthesis of *Moringa oleifera* leaf powder (MOLP) from East Java Indonesia: A preliminary study. In *AIP Conference Proceedings* (Vol. 2231, No. 1). AIP Publishing.
15. Mohd Rozi, N., Chandren, S., & Basar, N. (2025). *Garcinia mangostana* pericarp-assisted silver nanoparticles as a sustainable solution for tetracycline contaminants removal from wastewater. *Malaysian Journal of Fundamental and Applied Sciences, 21*(3), 2032–2044.
16. Parambath, S., Dao, A., Kim, H. Y., Zawahir, S., Alastruey-Izquierdo, A., Tacconelli, E., Govender, N., Oladele, R., Colombo, A., Sorrell, T., Ramon-Pardo, P., Fusire, T., Gigante, V., Sati, H., Morrissey, C. O., Alffenaar, J.-W., & Beardsley, J. (2024). *Candida albicans*—A systematic review to inform the World Health Organization fungal priority pathogens list. *Medical Mycology, 62*(6), myae045.
17. Razak, N. H. A., Din, S. M., Malek, N. A. N. N., Dagang, W. R. Z. W., Zawawi, N. A., & Chundawat, T. S. (2023). Antibacterial activity of biosynthesized green silver nanoparticles from *Orthosiphon aristatus* against marine bacteria. In *AIP Conference Proceedings* (Vol. 2634, No. 1, p. 020063). AIP Publishing LLC.
18. Rozhin, A., Batasheva, S., Kruychkova, M., Cherednichenko, Y., Rozhina, E., & Fakhrullin, R. (2021). Biogenic silver nanoparticles: Synthesis and application as antibacterial and antifungal agents. *Micromachines, 12*(12), 1480.
19. Sari, Y. P., Suchi, A. Q., & Nugroho, R. A. (2023). Biosynthesis and characterization of silver nanoparticles using single garlic callus extract (*Allium sativum* L.). *Malaysian Journal of Fundamental and Applied Sciences, 19*(4), 563–572.
20. Tailor, S., & Marwal, A. (2026). Bloom to bioactive: Environmentally benign biosynthesis and characterization of silver nanoparticles mediated by Mangifera indica flower bud extract and evaluation of their antibacterial and antifungal activity. *Russian Journal of Applied Chemistry*, *99*(3), 172-185.

21. Waiezi, S., Malek, N. A. N. N., Asraf, M. H., & Sani, N. S. (2023). Preparation, characterization, and antibacterial activity of green-biosynthesised silver nanoparticles using *Clinacanthus nutans* extract. *Biointerface Research in Applied Chemistry, 13*, 171.